

Quantum paramagnetic ground states on the honeycomb lattice and field-induced Néel order

R. Ganesh,¹ D. N. Sheng,² Young-June Kim,¹ and A. Paramekanti^{1,3}

¹*Department of Physics, University of Toronto, Toronto, Ontario, Canada M5S 1A7*

²*Department of Physics and Astronomy, California State University, Northridge, California 91330, USA*

³*Canadian Institute for Advanced Research, Toronto, Ontario, Canada M5G 1Z8*

(Received 13 December 2010; published 18 April 2011; publisher error corrected 13 June 2011)

$\text{Bi}_3\text{Mn}_4\text{O}_{12}(\text{NO}_3)$ is a recently synthesized spin-3/2 bilayer honeycomb antiferromagnet which behaves as a spin liquid down to very low temperatures. Beyond a magnetic field of about 5 T, it develops long-range Néel order. Motivated by this observation, we have studied spin- S Heisenberg models with next neighbor frustrating interactions as well as bilayer couplings on the honeycomb lattice. For a model with frustrating second-neighbor exchange, J_2 , we use a Lindemann-like criterion within spin-wave theory to show that Néel order melts beyond a critical J_2 . The critical J_2 is found to increase in the presence of a magnetic field, implying the existence of a field-induced paramagnet-Néel transition over a range of parameters. For the bilayer model, we use a spin- S generalization of bond operator mean-field theory to show that there is a Néel-dimer transition for various spin values with increasing bilayer coupling and that the resulting interlayer dimer state undergoes a field-induced transition into a state with transverse Néel order. Motivated by a broader interest in such paramagnets, we have also studied a spin-3/2 model which interpolates between the nearest-neighbor Heisenberg model and the Affleck-Kennedy-Lieb-Tasaki (AKLT) parent Hamiltonian. Using exact diagonalization, we have found that there is a single Néel-AKLT quantum phase transition in this model. Computing the fidelity susceptibility and assuming a transition in the $O(3)$ universality class, we have located the critical point of this model. In addition, we have obtained the spin gap of the AKLT parent Hamiltonian. Our numerics indicate that the AKLT state also undergoes a field-induced Néel ordering transition. We discuss implications of some of our results for experiments on $\text{Bi}_3\text{Mn}_4\text{O}_{12}(\text{NO}_3)$ and for numerics on the honeycomb lattice Hubbard model.

DOI: [10.1103/PhysRevB.83.144414](https://doi.org/10.1103/PhysRevB.83.144414)

PACS number(s): 75.10.Jm, 75.10.Kt, 75.30.Ds

The interplay of quantum mechanics and frustrated interactions in quantum magnets leads to a variety of remarkable phases including spin-liquid Mott insulators, valence bond crystals, and Bose-Einstein condensates of magnons.¹ Recently, there has been tremendous interest in novel paramagnetic ground states on the honeycomb lattice. A quantum Monte Carlo study of the repulsive electronic Hubbard model on the honeycomb lattice has uncovered a spin-liquid ground state² leading to a flurry of studies of honeycomb lattice spin liquids.^{3–5} Another interesting honeycomb lattice paramagnet is the $S = 3/2$ Affleck-Kennedy-Lieb-Tasaki (AKLT) state.^{6–8} Such an AKLT state is most easily understood by viewing each spin-3/2 as being composed of three spin-1/2 moments symmetrized on site, with each spin-1/2 moment forming a singlet with one neighbor, leading to a ground state which respects all lattice symmetries. This state has been suggested as an entanglement resource for universal quantum computation.⁹ Furthermore, an optical analog of the one-dimensional AKLT state has been realized in recent experiments,¹⁰ raising hopes for alternative realizations of AKLT states in higher dimensions.

Interest in honeycomb lattice quantum paramagnets also stems from experiments¹¹ on $\text{Bi}_3\text{Mn}_4\text{O}_{12}(\text{NO}_3)$. The crystal field of the MnO_6 octahedra, together with strong Hund's coupling, leads to Heisenberg-like spin-3/2 moments on the Mn^{4+} ions which form a bilayer honeycomb lattice. Despite the bipartite structure, and a large antiferromagnetic Curie-Weiss constant $\Theta_{\text{CW}} \approx -257\text{K}$, this system shows no magnetic order¹¹ (or any other phase transition) down to $T \sim 1\text{K}$. This observation hints at frustrating interactions which may lead to interesting paramagnetic ground states.^{12–17}

Neutron scattering experiments¹⁸ on powder samples of $\text{Bi}_3\text{Mn}_4\text{O}_{12}(\text{NO}_3)$ in zero magnetic field indicate that there are short-range spin correlations in this material, with some antiferromagnetic coupling between the two layers forming the bilayer, but negligible interactions between adjacent bilayers. Remarkably, applying a critical magnetic field, $B_c \sim 6\text{T}$, leads to sharp Bragg spots consistent with three-dimensional (3D) Néel order.¹⁸

Motivated by this broad interest in honeycomb lattice quantum paramagnets, we study various Heisenberg models with additional exchange interactions chosen to frustrate Néel order. We also consider the effect of a magnetic field on the paramagnetic states which result from the destruction of Néel order. We show that applying a critical magnetic field to these paramagnetic ground states leads to a transition into a state with long-range Néel order in the plane transverse to the applied field, which allows us to make connections with ongoing experiments and predictions for numerical studies of such paramagnetic states.

We begin with a study of a model with nearest-neighbor (J_1) and frustrating second-neighbor (J_2) exchange interactions. Such a model is relevant to $\text{Bi}_3\text{Mn}_4\text{O}_{12}(\text{NO}_3)$ as well as numerical studies of the honeycomb lattice Hubbard model. At the classical level, it is known that such frustration leads to the Néel state becoming unstable for $J_2/J_1 > 1/6$. In a quantum model with finite S , Néel order is likely to melt for smaller J_2/J_1 , although the nature of the resulting paramagnetic ground state is not known. Sidestepping the issue of what state results from quantum melting, we study the magnetic field dependence of the critical J_2/J_1 required to destroy the Néel order. Using spin-wave theory, we show that a nonzero

magnetic field enhances the critical J_2/J_1 , opening up a regime where applying a critical field to the non-Néel state yields long-range Néel order.

Next, motivated by the fact that $\text{Bi}_3\text{Mn}_4\text{O}_{12}(\text{NO}_3)$ consists of stacked bilayers, we study a bilayer honeycomb magnet where the interlayer exchange interaction competes with the intralayer coupling. Using a spin- S generalization¹⁹ of the bond operator formalism,²⁰ we show that a sufficiently strong bilayer coupling leads to an interlayer valence-bond solid (VBS) state. We obtain the Néel-to-interlayer VBS transition point for various spin values, which could be tested using quantum Monte Carlo numerics, as well as the triplon dispersion in the interlayer VBS. We show that the presence of a magnetic field strong enough to overcome the spin gap, results in the interlayer VBS undergoing a Bose condensation transition into a state with long-range Néel order in the plane transverse to the applied field. Remarkably, we find that the transition to the interlayer VBS state for spin-1/2 occurs even if the interlayer exchange is weaker than the interplane exchange, suggesting that spin-1/2 bilayer honeycomb magnets might be a promising system to realize this VBS state. For $S = 3/2$, we find that the VBS state is only realized at large interlayer couplings, $J_c/J_1 \gtrsim 3$.

Recent attempts to determine the relevant exchange couplings in $\text{Bi}_3\text{Mn}_4\text{O}_{12}(\text{NO}_3)$ indicate the presence of longer-range couplings in the honeycomb plane.^{21,22} Furthermore, while Ref. 21 focused on a single layer, the *ab initio* results of Ref. 22 provide evidence for quite strong interlayer couplings. In the light of these reports, our work on the J_1 - J_2 model and the bilayer model is perhaps quite relevant to understand the physics of $\text{Bi}_3\text{Mn}_4\text{O}_{12}(\text{NO}_3)$. We note, however, that Refs. 21 and 22 disagree on the sign of the further neighbor couplings within the honeycomb layer, suggesting the need for further work on this issue.

Finally, from the viewpoint of broader theoretical interest, we explore a generalized spin-3/2 model including biquadratic and bicubic spin interactions which interpolates between a Heisenberg model and the parent Hamiltonian of the $S = 3/2$ AKLT state. Using exact diagonalization, we obtain the spin-gap of the AKLT parent Hamiltonian. We also compute the fidelity susceptibility²³ of this model, and find that it indicates a direct AKLT-Néel transition. Using the fidelity susceptibility and the assumption of an $O(3)$ critical point, we identify the AKLT-Néel transition point in this model. By comparing the spin correlations in the singlet ground state and in the ground state with $S_z^{\text{tot}} = 1$, which are obtained using the exact diagonalization, we argue that a magnetic field applied to the AKLT state results in a transition to transverse Néel order.

I. SECOND-NEIGHBOR EXCHANGE

It has been suggested that the absence of Néel order in $\text{Bi}_3\text{Mn}_4\text{O}_{12}(\text{NO}_3)$ is linked to non-negligible further neighbor interactions.¹¹ We therefore study a minimal Hamiltonian,

$$H = J_1 \sum_{\langle ij \rangle} \mathbf{S}_i \cdot \mathbf{S}_j + J_2 \sum_{\langle\langle ij \rangle\rangle} \mathbf{S}_i \cdot \mathbf{S}_j - B \sum_i S_i^z, \quad (1)$$

where $\langle \cdot \rangle$ and $\langle\langle \cdot \rangle\rangle$ denote nearest- and next-nearest-neighbor bonds, respectively, and B is a Zeeman field. Let us begin with a classical analysis valid for $S = \infty$. When $J_2 = B = 0$, the

ground state has collinear Néel order. For $J_2 = 0$ and $B \neq 0$, the spins in the Néel state start off in the plane perpendicular to the applied field and cant along the field direction until they are fully polarized for $B > 6J_1S$. For $B < 6J_1S$, the spin components transverse to the magnetic field have staggered Néel order for $J_2 < J_1/6$; for $J_2 > J_1/6$, this gives way to a one-parameter family of degenerate (canted) spirals.¹⁵

Incorporating quantum fluctuations is likely to lead to melting of Néel order even for $J_2 < J_1/6$. Such fluctuations are also likely to completely suppress the classical spiral order.¹⁵ Using spin-wave theory, we argue here that a small nonzero B enhances the stability of the Néel order compared to the zero field case. (i) For small nonzero B , spin canting leads to a small decrease, $\propto B^2$, in the classical staggered magnetization transverse to the field. (ii) On the other hand, one of the two magnon modes (labeled $\Omega_{\mathbf{k}}^{\pm}$) acquires a nonzero gap $\propto B$ at the Γ point as shown in Fig. 2. This suppresses low-lying spin-wave fluctuations. For $B \ll 6J_1S$, the latter effect overwhelms the former, leading to enhanced stability of Néel order.

Let us discuss this stability line within spin-wave theory. When $J_2 < J_1/6$ and $B < 6J_1S$, Néel ordering is in the plane perpendicular to the magnetic field, but the spins also uniformly cant in the direction of applied field, to maximally gain Zeeman energy. The classical spin state can thus be characterized by $\mathbf{S}_{\mathbf{r}} = S(\pm \cos \chi, 0, \sin \chi)$ on the two sublattices. We now define new spin operators, denoted by $\mathbf{T}_{i,\alpha}$, via a sublattice-dependent local spin rotation

$$\begin{pmatrix} T_{i,\alpha}^x \\ T_{i,\alpha}^y \\ T_{i,\alpha}^z \end{pmatrix} = \begin{pmatrix} \sin \chi & 0 & (-)^{\alpha+1} \cos \chi \\ 0 & 1 & 0 \\ (-)^{\alpha} \cos \chi & 0 & \sin \chi \end{pmatrix} \begin{pmatrix} S_{i,\alpha}^x \\ S_{i,\alpha}^y \\ S_{i,\alpha}^z \end{pmatrix}, \quad (2)$$

where $\alpha = 1, 2$, is a sublattice index and i sums over each unit cell.

The ground state has all spins pointing toward the new local- S^z axis. To study spin-wave fluctuations, we rewrite the T operators in terms of Holstein-Primakoff bosons as follows:

$$\begin{aligned} T_{i,\alpha}^z &= S - b_{i,\alpha}^{\dagger} b_{i,\alpha}, \\ T_{i,\alpha}^x &= \sqrt{\frac{S}{2}} (b_{i,\alpha} + b_{i,\alpha}^{\dagger}), \\ T_{i,\alpha}^y &= \frac{1}{i} \sqrt{\frac{S}{2}} (b_{i,\alpha} - b_{i,\alpha}^{\dagger}). \end{aligned}$$

The Hamiltonian can now be rewritten as $H \approx E_{\text{Cl}} + H_{\text{qu}}$. The classical energy E_{Cl} is proportional to S^2 , and the leading order quantum correction, H_{qu} , is of order S . We get the value of the canting angle χ by demanding that terms of order $S^{3/2}$, which are linear in the boson operators, should vanish, which yields

$$\sin \chi = \frac{B}{6J_1S}. \quad (3)$$

The classical energy is given by

$$\frac{E_{\text{Cl}}}{NS^2} = -\frac{3}{2}J_1 \cos 2\chi + \frac{3}{2}J_2 - \frac{B}{S} \sin \chi. \quad (4)$$

where N is the number of sites in the honeycomb lattice. We take the magnetic field B to be of order S , so that the Zeeman

term $-BS_i^z$ is treated on the same level as the exchange terms $J_{ij}\mathbf{S}_i \cdot \mathbf{S}_j$. The leading quantum correction is given by

$$H_{\text{qu}} = -\frac{3NS}{2}J_1 \cos 2\chi + 3NSJ_2 - \frac{NB}{2} \sin \chi + \sum_{\mathbf{k}>0} \psi_{\mathbf{k}}^\dagger H_{\mathbf{k}} \psi_{\mathbf{k}}, \quad (5)$$

where

$$\psi_{\mathbf{k}} = \begin{pmatrix} b_{\mathbf{k},1} \\ b_{\mathbf{k},2} \\ b_{-\mathbf{k},1}^\dagger \\ b_{-\mathbf{k},2}^\dagger \end{pmatrix}; \quad H_{\mathbf{k}} = S \times \begin{pmatrix} I_{\mathbf{k}} & F_{\mathbf{k}} & 0 & G_{\mathbf{k}} \\ F_{\mathbf{k}}^* & I_{\mathbf{k}} & G_{\mathbf{k}}^* & 0 \\ 0 & G_{\mathbf{k}} & I_{\mathbf{k}} & F_{\mathbf{k}} \\ G_{\mathbf{k}}^* & 0 & F_{\mathbf{k}}^* & I_{\mathbf{k}} \end{pmatrix}, \quad (6)$$

with

$$I_{\mathbf{k}} = 3J_1 \cos 2\chi - 6J_2 + 2J_2 \{\cos k_a + \cos k_b + \cos(k_a + k_b)\} + \frac{B}{S} \sin \chi, \quad F_{\mathbf{k}} = J_1 \gamma_{\mathbf{k}} \sin^2 \chi \equiv |F_{\mathbf{k}}| e^{i\eta_{\mathbf{k}}},$$

$$G_{\mathbf{k}} = -J_1 \gamma_{\mathbf{k}} \cos^2 \chi,$$

where $\gamma_{\mathbf{k}} = 1 + e^{-i\mathbf{k}\cdot\hat{b}} + e^{-i\mathbf{k}\cdot(\hat{a}+\hat{b})}$, with unit vectors $\hat{a} = \hat{x}$, $\hat{b} = -\hat{x}/2 + \sqrt{3}\hat{y}/2$. This Hamiltonian can be diagonalized by a bosonic Bogoliubov transformation. The eigenvalues are given by

$$\Omega_{\mathbf{k}}^\pm = S \sqrt{(I_{\mathbf{k}} \pm |F_{\mathbf{k}}|)^2 - |G_{\mathbf{k}}|^2}. \quad (7)$$

The Bogoliubov transformation matrix to rotate into the quasiparticle operators is given by

$$P = \begin{pmatrix} U_{2 \times 2} & 0 \\ 0 & U_{2 \times 2} \end{pmatrix} \begin{pmatrix} C_{2 \times 2} & S_{2 \times 2} \\ S_{2 \times 2} & C_{2 \times 2} \end{pmatrix},$$

where

$$U_{2 \times 2} = \frac{1}{\sqrt{2}} \begin{pmatrix} -e^{i\eta_{\mathbf{k}}} & e^{i\eta_{\mathbf{k}}} \\ 1 & 1 \end{pmatrix}; \quad (8)$$

$$C_{2 \times 2} = \begin{pmatrix} \cosh \theta & 0 \\ 0 & \cosh \phi \end{pmatrix}; \quad S_{2 \times 2} = \begin{pmatrix} \sinh \theta & 0 \\ 0 & \sinh \phi \end{pmatrix}, \quad (9)$$

where the angles θ and ϕ are given by

$$\tanh 2\theta = \frac{|G_{\mathbf{k}}|}{I_{\mathbf{k}} - |F_{\mathbf{k}}|}, \quad \tanh 2\phi = \frac{-|G_{\mathbf{k}}|}{I_{\mathbf{k}} + |F_{\mathbf{k}}|}. \quad (10)$$

The matrix P preserves the commutation relations of the bosonic operators and diagonalizes the Hamiltonian, giving $P^\dagger H P = \text{Diag}\{\Omega_{\mathbf{k}}^-, \Omega_{\mathbf{k}}^+, \Omega_{\mathbf{k}}^-, \Omega_{\mathbf{k}}^+\}$. Figure 1 shows a plot of the magnon dispersion in the Néel state at nonzero B along certain high-symmetry directions in the Brillouin zone.

The strength of long-range magnetic order can be calculated in this new basis. For example, the in-plane component of the spin is given by

$$\frac{1}{N} \sum_i \langle S_{i,\alpha=1}^x \rangle = (S + 1/2) \cos \chi - \frac{\cos \chi}{N} \times \sum_{\mathbf{k}>0} [\cosh 2\theta \{1 + 2n_B(\Omega_{\mathbf{k},-})\} + \cosh 2\phi \{1 + 2n_B(\Omega_{\mathbf{k},+})\}], \quad (11)$$

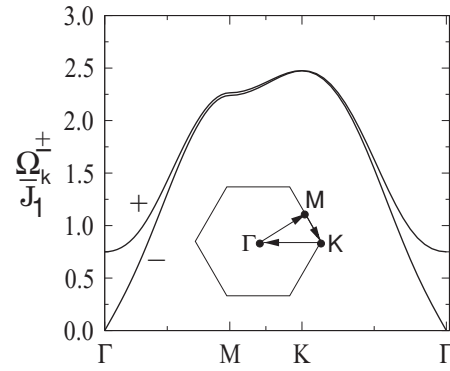


FIG. 1. Dispersion of magnon modes $\Omega_{\mathbf{k}}^\pm$ in the J_1 - J_2 model along depicted path in the Brillouin zone for $J_2 = 0.15J_1$, $S = 3/2$, and $B = 0.5J_1S$.

where $n_B(\cdot)$ denotes the Bose distribution function. For $T = 0$, we can simply use the 2D Hamiltonian to compute this renormalized order parameter. For $T \neq 0$, we have to take into account a small coupling along the third dimension to allow for a stable magnetically ordered state. For a layered system with very weak interlayer coupling, we can use the 2D Hamiltonian together with an infrared cutoff Λ , which is of the order of the interlayer coupling. In this case, spin-wave modes with energies greater than Λ appear to be 2D spin waves. On the other hand, modes with energies below Λ can be dropped as their contribution will be suppressed by phase-space factors in the 3D problem. In our numerics, we impose this infrared cutoff by simply restricting ourselves to a finite system size. Finite size automatically cuts off long wavelength modes with $k < k_c \sim 2\pi/\sqrt{N}$. In our calculations, we have restricted our system size to $2 \times 120 \times 120$ spins. This corresponds to $k_c \sim 0.05$, leading to an infrared cutoff of $\Lambda \sim 0.04JS$.

As J_2 is increased from zero, fluctuations around the Néel state increase due to frustration. With increasing fluctuations, we expect the Néel state to melt when fluctuations become comparable to the magnitude of the ordered moment. To estimate the ‘‘melting curve,’’ we assume that the transverse spin components have Néel order along the S_x direction, and use a heuristic Lindemann-like criterion for melting: $\sqrt{\langle S_x^2 \rangle} - \langle S_x \rangle^2 > \alpha \langle S_x \rangle$. The expectation values are evaluated (using linear spin-wave theory) to order 1, even though the Hamiltonian has terms up to order S only.

We set $\alpha = 5$ since this leads to melting of Néel order for $S = 1/2$ at $J_2 \approx 0.08J_1$, in agreement with a recent variational Monte Carlo study by Clark *et al.*³ The resulting Néel melting curves, at zero and nonzero temperatures, are shown in Figs. 2 and 3.

As shown in Fig. 2 and its inset, quantum fluctuations at $B = 0$ lead to melting of Néel order even for $J_2 < J_1/6$ (i.e., before the classical destruction of Néel order). For nonzero B , the ‘‘melting point’’ moves toward larger J_2 , leading to a window of J_2 over which the quantum disordered liquid can undergo a field-induced phase transition to Néel order. The window of J_2 where such physics is operative appears to be small for $S = 3/2$; however, disorder effects, which tend to suppress the stiffness,²⁴ may enhance this regime. Furthermore, as seen from Fig. 3, the window of J_2 over which we expect field-induced Néel order is also enhanced at small

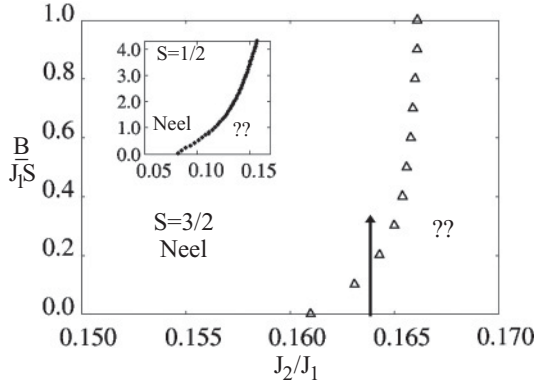


FIG. 2. $T = 0$ melting of Néel order for $S = 3/2$ in the B - J_2 plane (open triangles) obtained using a Lindemann-like criterion, $\sqrt{\langle S_x^2 \rangle - \langle S_x \rangle^2} = 5\langle S_x \rangle$. The region labeled “??” is a quantum disordered state—possibly a valence bond solid or a quantum spin liquid. Arrow depicts path along which one obtains a field-induced transition to Néel order. (Inset) A similar melting curve for $S = 1/2$.

nonzero temperatures. Finally, we expect field-induced Néel order even for $S = 1/2$ (see inset to Fig. 2).

Our results are consistent with recent neutron diffraction experiments¹⁸ on $\text{Bi}_3\text{Mn}_4\text{O}_{12}(\text{NO}_3)$, which find field-induced Néel order. Our results also explain recent Monte Carlo simulations of the classical J_1 - J_2 model¹⁶ with $B \neq 0$; if $J_2 = 0.175J_1$, as in the simulations, increasing B at a fixed temperature takes us closer to the melting curve, as seen from Fig. 3. This may lead to the numerically observed enhanced Néel correlations. Nevertheless, we expect that there will be no field-induced *long-range* Néel order for $J_2 = 0.175J_1$ in the classical model. Finally, the J_1 - J_2 model is a reasonable effective model of the insulating phase of the repulsive honeycomb lattice Hubbard model, and recent quantum Monte Carlo simulations find a paramagnetic (spin liquid) insulator over a range of repulsion strengths in this model. Our prediction of field induced Néel order in this paramagnet can be verified by including a magnetic field in these quantum Monte Carlo simulations.

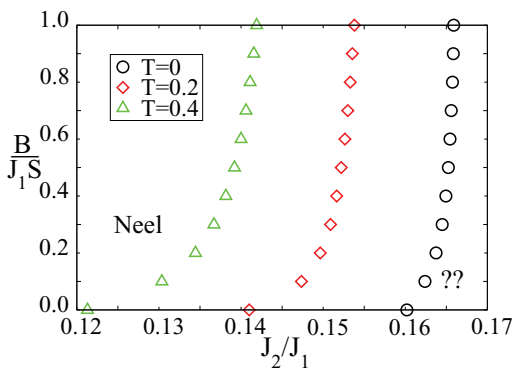


FIG. 3. (Color online) Melting of Néel order for $S = 3/2$ in the B - J_2 plane for depicted nonzero temperatures. To the left of the curve, there is stable canted Néel order. To the right, combined effects of quantum and thermal fluctuations melt the in-plane Néel order.

II. BILAYER HONEYCOMB LATTICE AND THE INTERLAYER DIMER STATE

The Mn sites in a unit cell of $\text{Bi}_3\text{Mn}_4\text{O}_{12}(\text{NO}_3)$ form an AA stacked bilayer honeycomb lattice. A recent density functional theory calculation²² estimates that the interlayer coupling within each bilayer is large, and may play an important role in determining the ground state. If the interplane antiferromagnetic exchange J_c is indeed large compared to J_1 , adjacent spins on the two layers could dimerize, leading to loss of Néel order. To study this interlayer VBS, we use the $J_1 - J_c$ model beginning from the limit of $J_1 = 0$; this leads to the spectrum $E_j = -J_c[S(S+1) - j(j+1)/2]$, with $j = 0, 1, \dots, 2S$ denoting the total spin state of the dimer. Restricting attention to the low-energy Hilbert space spanned by the singlet and the triplet states, we define generalized spin- S bond operators via: $|s\rangle = s^\dagger|0\rangle$, and $|\alpha\rangle = t_\alpha^\dagger|0\rangle$, where $|0\rangle$ is the vacuum, and $|\alpha(=x, y, z)\rangle$ are related to the m_j levels of the triplet by $|z\rangle = |m_j = 0\rangle$, $|x\rangle = (|m_j = -1\rangle - |m_j = 1\rangle)/\sqrt{2}$, and $|y\rangle = i(|m_j = -1\rangle + |m_j = 1\rangle)/\sqrt{2}$. Denoting the two spins constituting the dimer, by S_ℓ , with layer index $\ell = 0/1$, we obtain¹⁹

$$S_\ell^\alpha \approx (-1)^\ell \sqrt{\frac{S(S+1)}{3}} (s^\dagger t_\alpha + t_\alpha^\dagger s) - \frac{i}{2} \varepsilon_{\alpha\beta\gamma} t_\beta^\dagger t_\gamma, \quad (12)$$

together with the constraint $s^\dagger s + t_\alpha^\dagger t_\alpha = 1$ at each site.

To treat the effect of J_1 , we use bond operator mean-field theory,²⁰ which yields a reasonably accurate phase diagram for the spin-1/2 bilayer square lattice Heisenberg model.^{25,26} Assuming the singlets are condensed in the dimer solid, we replace $s^\dagger = s = \bar{s}$, and incorporate a Lagrange multiplier in the Hamiltonian which enforces $\langle t_\alpha^\dagger t_\alpha \rangle = 1 - \bar{s}^2$ on average. Let N be the number of spins in each honeycomb layer. We then obtain the Hamiltonian,

$$H = \sum_{\alpha, \mathbf{k} > 0} \Psi_{\mathbf{k}\alpha}^\dagger M_{\mathbf{k}} \Psi_{\mathbf{k}\alpha} + 2NC, \quad (13)$$

describing the dynamics of the triplets. Here $\Psi_{\mathbf{k}\alpha}^\dagger = (t_{\mathbf{k}\alpha 1}^\dagger t_{\mathbf{k}\alpha 2}^\dagger t_{-\mathbf{k}\alpha 1}^\dagger t_{-\mathbf{k}\alpha 2}^\dagger)$ (with 1,2 denoting the two sublattices in each layer) and the matrix $M_{\mathbf{k}}$ takes the form

$$M_{\mathbf{k}} = \begin{pmatrix} A_{\mathbf{k}} & B_{\mathbf{k}} & 0 & B_{\mathbf{k}} \\ B_{\mathbf{k}}^* & A_{\mathbf{k}} & B_{\mathbf{k}}^* & 0 \\ 0 & B_{\mathbf{k}} & A_{\mathbf{k}} & B_{\mathbf{k}} \\ B_{\mathbf{k}}^* & 0 & B_{\mathbf{k}}^* & A_{\mathbf{k}} \end{pmatrix}, \quad (14)$$

with

$$A_{\mathbf{k}} = J_c - \mu - J_c S(S+1), \quad (15)$$

$$B_{\mathbf{k}} = \frac{1}{3} \gamma_{\mathbf{k}} J_1 S(S+1) \bar{s}^2. \quad (16)$$

Here we have defined $\gamma_{\mathbf{k}} = 1 + e^{-i\mathbf{k}\cdot\hat{b}} + e^{-i\mathbf{k}\cdot(\hat{a}+\hat{b})}$, with unit vectors $\hat{a} = \hat{x}$, $\hat{b} = -\hat{x}/2 + \sqrt{3}\hat{y}/2$, and the constant

$$C = -\frac{\mu}{2}(\bar{s}^2 - 1) - \frac{3}{4}[J_c - \mu - J_c S(S+1)] - \frac{1}{2} J_c \bar{s}^2 S(S+1). \quad (17)$$

Diagonalizing this Hamiltonian leads to the ground-state energy per spin $E_g = \frac{3}{2N} \sum_{\mathbf{k} > 0} (\xi_{\mathbf{k}+} + \xi_{\mathbf{k}-}) + C$, where $\xi_{\mathbf{k}\pm} =$

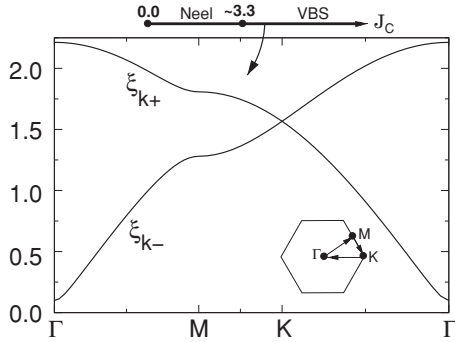


FIG. 4. Phase diagram of the $S = 3/2$ bilayer honeycomb model obtained using bond operator theory, and triplon dispersion along depicted path in the Brillouin zone within the interlayer VBS state for $J_c/J_1 = 3.8$ (in units where $J_1 = 1$).

$\sqrt{A_{\mathbf{k}}(A_{\mathbf{k}} \pm 2|B_{\mathbf{k}}|)}$. Setting $\partial E_g/\partial \bar{s}^2 = \partial E_g/\partial \mu = 0$, we obtain the mean-field values of \bar{s} and μ , which minimize the ground-state energy subject to the constraint. Solving these equations numerically, we find that the spin- S interlayer VBS is a stable phase for $J_c > J_*[S]$, where $J_*[3/2] \approx 3.3J_1$, $J_*[1] \approx 1.6J_1$, and $J_*[1/2] \approx 0.66J_1$. Quantum Monte Carlo studies of this model would be valuable in firmly establishing the value of $J_*[S]$ as a function of S . Figure 4 shows the triplon dispersion of the $S = 3/2$ interlayer VBS state at $J_c = 3.8J_1$ along high-symmetry cuts in the hexagonal Brillouin zone. For $J_c < J_*[S]$, or in the presence of a magnetic field which can close the spin gap in the VBS state for $J_c > J_*[S]$, the low-energy triplon mode at the Γ point condenses; its eigenvector is consistent with Néel order. For the field-induced Néel state, the Néel ordering is in the plane transverse to the applied magnetic field.

III. AKLT VALENCE BOND SOLID

A particularly interesting spin-gapped ground state of a magnet with spin- S atoms on a lattice of coordination number $z = 2S$, is an AKLT valence bond state. Each spin- S is viewed as being composed of $2S$ spin-1/2 moments symmetrized on site, with each spin-1/2 moment forming a singlet with one neighbor.⁶⁻⁸ It was originally proposed as an exact realization of Haldane's prediction of a spin-gapped ground state in 1D integer spin systems.²⁷ Assuming that the Mn^{4+} ions in $\text{Bi}_3\text{Mn}_4\text{O}_{12}(\text{NO}_3)$ mainly interact with the three neighboring spins in the same plane, this condition is satisfied with $S = 3/2$ and $z = 3$. The honeycomb lattice AKLT state has exponentially decaying spin correlations,⁷ and it is the exact, and unique, zero-energy ground state of the parent Hamiltonian $H_{\text{AKLT}} = \sum_{\langle ij \rangle} P_{i,j}^{(3)}$. Here $P_{i,j}^{(\ell)}$ denotes a projector on to total spin- ℓ for a pair of spins on nearest neighbor sites (i, j) . Denoting $T_{i,j} \equiv \mathbf{S}_i \cdot \mathbf{S}_j$, we find

$$P_{i,j}^{(3)} = \frac{11}{128} + \frac{243}{1440}T_{i,j} + \frac{116}{1440}T_{i,j}^2 + \frac{16}{1440}T_{i,j}^3. \quad (18)$$

We have investigated, using Exact Diagonalization (ED) on clusters with $N = 12-18$ spins, the phase diagram of a

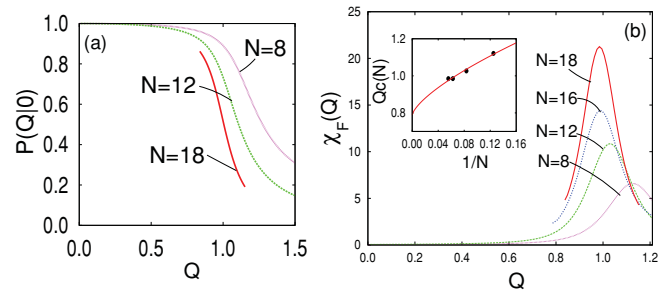


FIG. 5. (Color online) (a) Overlap $P(Q|0)$ of the ground state at Q with the Néel state ($Q = 0$) for various system sizes N , showing its rapid drop around the Néel-AKLT transition. (b) Fidelity susceptibility $\chi_F(Q)$ versus Q for various system sizes N , with the peak indicating the Néel-AKLT transition point $Q_c(N)$. (Inset) $Q_c(N)$ versus $1/N$, together with a fit $Q_c(N) = Q_c^\infty + bN^{-\frac{1}{2\nu}}$ (with a choice $\nu \approx 0.7$ assuming an $O(3)$ quantum phase transition in 2D), which leads to $Q_c^\infty \approx 0.8$.

generalized spin-3/2 model,

$$H_Q = (1 - Q) \sum_{\langle ij \rangle} \mathbf{S}_i \cdot \mathbf{S}_j + gQH_{\text{AKLT}}, \quad (19)$$

which interpolates between a Heisenberg model (at $Q = 0$) and gH_{AKLT} (at $Q = 1$). We set $g = 1440/243$, so that the coefficient of $\mathbf{S}_i \cdot \mathbf{S}_j$ in H_Q is unity.

For $Q = 0$, our analysis of the finite size spectrum shows that the ground-state energy $E_g(N, S^{\text{tot}})$, as a function of total spin S^{tot} , varies as $S^{\text{tot}}(S^{\text{tot}} + 1)$, in agreement with the expected Anderson tower for a Néel ordered state. It is consistent with earlier work^{12,28,29} showing Néel order even for spin-1/2. To establish the Néel-AKLT transition as a function of Q , we study overlaps $P(Q|Q') = |\langle \Psi_g(Q) | \Psi_g(Q') \rangle|$ of the ground-state wave functions at Q and Q' . As shown in Fig. 5(a), the overlap $P(Q|0)$, of the ground-state wave function at Q with the Néel state at $Q' = 0$ is nearly unity for $Q \lesssim 0.8$, suggesting that the ground state in this regime has Néel character. For $0.8 \lesssim Q < 1.2$, we observe a dramatic drop of $P(Q|0)$ for all system sizes, which indicates a Néel-AKLT quantum phase transition.

To locate the transition more precisely, we compute the fidelity susceptibility²³ $\chi_F(Q) = 2[1 - P(Q|Q + \delta)]/\delta^2$, with $\delta \rightarrow 0$, which measures the change of the wave function when $Q \rightarrow Q + \delta$. Figure 5(b) shows a plot of $\chi_F(Q)$ (with $\delta = 0.005$). We observe a peak in $\chi_F(Q)$ which indicates a phase transition; this peak shifts and grows sharper with increasing N . Assuming the thermodynamic transition is at Q_c^∞ and that the peak position $Q_c(N)$ satisfies the scaling relation $[Q_c(N) - Q_c^\infty] \sim N^{-1/2\nu}$, with $\nu \approx 0.7$ for an $O(3)$ quantum phase transition^{25,30} corresponding to triplon condensation, we estimate $Q_c^\infty \approx 0.8$. Further work is necessary to confirm the nature of the transition.

The spin gap of H_Q , $\Delta_s(N) = E_g(N, S^{\text{tot}} = 1) - E_g(N, S^{\text{tot}} = 0)$ is plotted in Fig. 6(a) for various Q as a function of $1/N$. Assuming a finite size scaling form $\Delta_s(N) = \Delta_s^\infty + b/N$, we find a small value for Δ_s^∞ for $Q = 0.0, 0.4$, consistent with a gapless Néel state, while for $Q = 0.9, 1.0$ we see a robust spin gap as $1/N \rightarrow 0$. At the AKLT point ($Q = 1$), we estimate $\Delta_s^\infty \approx 0.6$. Given our scaling factor g , this yields a value of ≈ 0.1 for the spin gap of H_{AKLT} .

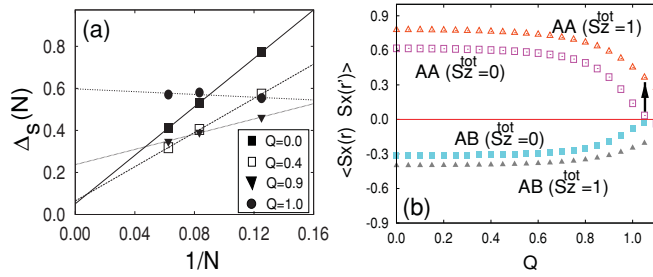


FIG. 6. (Color online) (a) Spin gap, $\Delta_s(N)$, versus $1/N$ for various Q , with fits to the form $\Delta_s(N) = \Delta_s^\infty + b/N$. The small values of Δ_s^∞ for $Q = 0.0, 0.4$ are consistent with a gapless Néel state. For $Q = 0.9, 1.0$, the data are consistent with a robust spin gap Δ_s^∞ . (b) S_x -spin correlations between distant sites on the same (AA) and opposite (AB) sublattices for $N = 16$ system. The spin correlation is Néel-like (\pm) for $Q < 1$ in the $S_z^{\text{tot}} = 0$ ground state; in the spin-gapped AKLT state at $Q \gtrsim 1$, it is short-ranged and weak in the $S_z^{\text{tot}} = 0$ ground state but it is strongly enhanced (see arrow) in the lowest lying state with $S_z^{\text{tot}} = 1$.

Since the spin gap is finite for $Q > Q_c$, we expect that applying a critical field $B_c \propto \Delta_s$ will lead to a phase transition; the correlation functions of the lowest-lying $S_z^{\text{tot}} = 1$ state at zero field will then reflect the correlations of the ground state for $B_z > B_c$. We plot, in Fig. 6(b), the spin correlations on two maximally separated sites (for $N = 16$) as a function of Q and make the following observations. (i) For $S_z^{\text{tot}} = 0$, the ground state also has $S^{\text{tot}} = 0$, and $\langle S_x(i)S_x(j) \rangle = \langle S_z(i)S_z(j) \rangle$ due to spin-rotational invariance. At long distance, the spin correlation is strong in the Néel phase but drops rapidly to small values upon entering the AKLT state. (ii) In the $S_z^{\text{tot}} = 1$ sector, $\langle S_z(i)S_z(j) \rangle \neq \langle S_x(i)S_x(j) \rangle$. Remarkably, in the lowest-lying state in this sector, as opposed to the $S^{\text{tot}} = 0$ ground state, we find a strong enhancement of (only) transverse correlations $\langle S_x(i)S_x(j) \rangle$ between distant sites in the AKLT state; this finite-size result suggests that the AKLT state will undergo, beyond a critical field, a transition into a state with in-plane Néel order.

IV. DISCUSSION

Motivated by recent theoretical and experimental work on honeycomb lattice paramagnetic states, we have studied

various Heisenberg models with competing interactions. The models we have studied have quantum paramagnetic ground states that undergo field-induced phase transitions to Néel order. In principle, if such competing states are thought to occur in any material, such as in $\text{Bi}_3\text{Mn}_4\text{O}_{12}(\text{NO}_3)$, detailed NMR studies of isolated nonmagnetic impurities substituted for Mn may help distinguish between these states. For a material with $S = 3/2$ moments, the interlayer VBS would have an impurity-induced $S = 3/2$ local moment on the neighboring site in the adjacent layer. The AKLT state would nucleate three $S = 1/2$ moments on neighboring sites in the same plane, while spinless impurities in spin-gapped Z_2 fractionalized spin liquids,³⁻⁵ do not generically lead to local moments. Sharply dispersing triplet excitations expected in valence bond solids discussed here could be looked for using single-crystal inelastic neutron scattering; by contrast, a spin liquid may not possess such sharp modes. Specific heat experiments in a magnetic field could test for Bose-condensation of triplet excitations as a route to Néel order, which we think describes the transition of the AKLT and the interlayer dimer paramagnets.

If the ground state of $\text{Bi}_3\text{Mn}_4\text{O}_{12}(\text{NO}_3)$ is a valence bond solid, disorder and Dzyaloshinskii-Moriya couplings (permitted by the bilayer structure) may be responsible for the observed nonzero low temperature susceptibility. Finally, dimer crystals with broken symmetry could also be candidate ground states in $\text{Bi}_3\text{Mn}_4\text{O}_{12}(\text{NO}_3)$; if this is the case, disorder must be responsible for wiping out the thermal transition expected of such crystals. These are interesting directions for future research.

ACKNOWLEDGMENTS

We thank J. Alicea, M. Azuma, L. Balents, G. Baskaran, E. Berg, D. Dalidovich, Y. B. Kim, M. Matsuda, and O. Starykh for discussions. This research was supported by the Canadian NSERC (R.G., Y.J., A.P.), an Ontario Early Researcher Award (R.G., A.P.), and US NSF Grants No. DMR-0906816 and No. DMR-0611562 (D.N.S.). R.G. and A.P. acknowledge the hospitality of the Physics Department, Indian Institute of Science, and the International Center for Theoretical Sciences while this paper was being written.

¹L. Balents, *Nature (London)* **464**, 199 (2010); R. Moessner and A. P. Ramirez, *Phys. Today* **59**, 24 (2006); T. Giamarchi, Ch. Rüegg, and O. Tchernyshyov, *Nat. Phys.* **4**, 198 (2008).

²Z. Y. Meng, T. C. Lang, S. Wessel, F. F. Assaad, and A. Muramatsu, *Nature (London)* **464**, 847 (2010).

³F. Wang, *Phys. Rev. B* **82**, 024419 (2010).

⁴Y.-M. Lu and Y. Ran, e-print [arXiv:1007.3266](https://arxiv.org/abs/1007.3266) (to be published).

⁵B. K. Clark, D. A. Abanin, and S. L. Sondhi, e-print [arXiv:1010.3011](https://arxiv.org/abs/1010.3011) (to be published).

⁶I. Affleck, T. Kennedy, E. H. Lieb, and H. Tasaki, *Phys. Rev. Lett.* **59**, 799 (1987); *Commun. Math. Phys.* **115**, 477 (1988).

⁷D. P. Arovas, A. Auerbach, and F. D. M. Haldane, *Phys. Rev. Lett.* **60**, 531 (1988).

⁸T. Kennedy, E. H. Lieb, and H. Tasaki, *J. Stat. Phys.* **53**, 383 (1988).

⁹J. Cai, A. Miyake, W. Dür, and H. J. Briegel, *Phys. Rev. A* **82**, 052309 (2010); T.-C. Wei, I. Affleck, and R. Raussendorf, *Phys. Rev. Lett.* **106**, 070501 (2011); A. Miyake, e-print [arXiv:1009.3491](https://arxiv.org/abs/1009.3491) (to be published).

¹⁰J. Lavoie, R. Kaltenbaek, B. Zeng, S. D. Bartlett, and K. J. Resch, *Nat. Phys.* **6**, 850 (2010).

¹¹O. Smirnova, M. Azuma, N. Kumada, Y. Kusano, M. Matsuda, Y. Shimakawa, T. Takei, Y. Yonesaki, and N. Kinomura, *J. Am. Chem. Soc.* **131**, 8313 (2009); S. Okubo, F. Elmasry, W. Zhang, M. Fujisawa, T. Sakurai, H. Ohta, M. Azuma, O. A. Sumirnova, and N. Kumada, *J. Phys.: Conf. Ser.* **200**, 022042 (2010).

- ¹²J. B. Fouet, P. Sindzingre, and C. Lhuillier, *Eur. Phys. J. B* **20**, 241 (2001).
- ¹³A. Mattsson, P. Fröjdh, and T. Einarsson, *Phys. Rev. B* **49**, 3997 (1994).
- ¹⁴K. Takano, *Phys. Rev. B* **74**, 140402 (2006).
- ¹⁵A. Mulder, R. Ganesh, L. Capriotti, and A. Paramekanti, *Phys. Rev. B* **81**, 214419 (2010).
- ¹⁶S. Okumura, H. Kawamura, T. Okubo, and Y. Motome, *J. Phys. Soc. Jpn.* **79**, 114705 (2010).
- ¹⁷H. Mosadeq, F. Shahbazi, and S. A. Jafari, e-print [arXiv:1007.0127](https://arxiv.org/abs/1007.0127) (unpublished).
- ¹⁸M. Matsuda, M. Azuma, M. Tokunaga, Y. Shimakawa, and N. Kumada, *Phys. Rev. Lett.* **105**, 187201 (2010).
- ¹⁹B. Kumar, *Phys. Rev. B* **82**, 054404 (2010).
- ²⁰S. Sachdev and R. N. Bhatt, *Phys. Rev. B* **41**, 9323 (1990).
- ²¹H. Wadati, K. Kato, Y. Wakisaka, T. Sudayama, D. G. Hawthorn, T. Z. Regier, N. Onishi, M. Azuma, Y. Shimakawa, T. Mizokawa, A. Tanaka, and G. A. Sawatzky, e-print [arXiv:1101.2847](https://arxiv.org/abs/1101.2847) (to be published).
- ²²H. C. Kandpal and J. van den Brink, e-print [arXiv:1102.3330](https://arxiv.org/abs/1102.3330) (to be published).
- ²³A. F. Albuquerque, F. Alet, C. Sire, and S. Capponi, *Phys. Rev. B* **81**, 064418 (2010).
- ²⁴A. Paramekanti, N. Trivedi, and M. Randeria, *Phys. Rev. B* **57**, 11639 (1998).
- ²⁵A. W. Sandvik and D. J. Scalapino, *Phys. Rev. Lett.* **72**, 2777 (1994).
- ²⁶Y. Matsushita, M. P. Gelfand, and C. Ishii, *J. Phys. Soc. Jpn.* **68**, 247 (1999).
- ²⁷F. D. M. Haldane, *Phys. Lett. A* **93**, 464 (1983); *Phys. Rev. Lett.* **50**, 1153 (1983).
- ²⁸J. D. Reger, J. A. Riera, and A. P. Young, *J. Phys. Condens. Matter* **1**, 1855 (1989).
- ²⁹Z. Nourbakhsh, F. Shahbazi, and S. A. Jafari, and G. Baskaran, *J. Phys. Soc. Jpn.* **78**, 054701 (2009); H. Mosadeq, F. Shahbazi, and S. A. Jafari, e-print [arXiv:1007.0127](https://arxiv.org/abs/1007.0127) (to be published).
- ³⁰P. Peczak, A. M. Ferrenberg, and D. P. Landau, *Phys. Rev. B* **43**, 6087 (1991).